Analysis Resonant Compensation for Wireless Power Transfer via Magnetic Coupling

Qiang Zhao, Anna Wang, Hao Wang

College of Information Science and Engineering,
Northeastern University, Shenyang 110819, Liaoning, China

Abstract
In recent years, based on near-field magnetic resonance coupling wireless energy transmission technology has been widespread concern. Compared with conventional inductive power transfer of the far-field region, it overcomes the shortcomings of distance and efficiency of electrical energy, and a new transmission, has important research value. To improve the transfer efficiency when the coil parameters and distance changes, a resonant compensation topologies for WPT are analyzed and the expressions of the transfer efficiency are deduced. It is pointed out that the transfer quality factor and the coupling coefficient are two important factors of achieving high transfer efficiency. In this paper, the influence of these to voltage gain, current gain, and the efficiency of transfer for the bilateral compensation in WPT are studied in detail, and the relationship of quality factor, coil parameters, frequency is built. In addition, bilateral compensation will increse the order of system, and it will result to have multiple resonance frequency points in the system, that is, the phenomenon of frequency bifurcation occurs. The formula of frequency bifurcation of system has been deduced, it can avoid the stability problems of the system due to frequency bifurcation.The simulation results show that the quality factor and coupling coefficient have a different effect on the topological structure. The structure of primary series secondary series has nothing to do with them, and efficiency was less affected when operating frequency deviating slightly from the resonant frequency.
Key words: WIRELESS POWER TRANSFER, MAGNETIC COUPLING RESONANCE, QUALITY FACTOR, TRANSFER EFFICIENCY, BIFURCATION

Introduction

Resonant magnetic coupling wireless power transmission technology is a frontier topic in the power transmission field. It uses a coupled-mode theory, power electronics, high-frequency electronic technology, electromagnetic field technology and other disciplines, and enables supply power to the mobile device from a distance [1].This technology can effectively overcome the device moves inflexible, environment unsightly, prone to contact sparks, power lines and other issues exposed the existence of traditional power [2], which in turn eliminates the safety problems exist in the traditional power supply, so that the

whole process more secure power supply. This technology not only in electric vehicles, aerospace, military, oil mines, and underwater operations has important applications, but also has a wide application in household appliances, medical devices[3]–[5]. The wireless energy transmission technology will be applied in various fields in the future will be more widely with the in-depth study. But at present the wireless energy transmission technology is not very mature and many problems still exist in the development process, including the coupling coefficient [6], The frequency stability and splitting of the energy transfer process [7], Stability of transmission current and voltage [8], electromagnetic compatibility [9], impedance matching [10], transmission power and other issues, which are urgently needed to solve the problem. Wireless power transmission can be accomplished by two different technologies depending on the operating frequencies; near- or far-field power transfer systems. Far-field wireless power transfer systems can be categorized into two systems depending on the operating principle; directional radiation antenna (microwave antennas) and power-beaming by visible light (laser and photovoltaic cells). Near-field wireless power transfer systems can also be categorized into two different systems depending on the coupling medium; electric field coupling (capacitive coupling) and magnetic field coupling (inductive coupling).The surrounding area of a transmitting antenna can be categorized into three sub-regions depending on the distance from the antenna: reactive near-field region, radioactive near-field region, and far-field region. According to Balanis [11], the reactive near-field region is the zone where the reactive fields and their oscillating energy are predominant. Coupled magnetic resonance was reported in Science [12]. This technology showed the potential to deliver power with higher efficiency than far-field approaches, and at longer ranges than traditional inductively coupled schemes [12].

In previous research works, there have been many groups and areas that have benefited from research in the area of near field magnetic resonant coupling. The majority of work has been in the area of either electromagnetic, optics, or physics, with an emphasis in a variety of applications. Similar experiments have been improved upon for a variety of applications. In [13], the compensated capacitors are in serious or in shunt with the primary side and secondary side, both simulations and experiments show that better transfer efficiency has been achieved because higher frequency was adopted. In [14], A circuit model is presented along with a derivation of key system concepts such as frequency splitting, the maximum operating distance (critical coupling), and the behavior of the system as it becomes under-coupled. In [15], the transferred power was reported to be maximized at the resonant frequencies of the input impedance. However, ref [15] only dealt with the two-coil structure and was aimed at maximizing the transferred power, and there was no reference of the quality factor characteristic, which could not be neglected in maximizing efficiency. In [16], the coupling between the source loop (load loop) and the Tx coil (Rx coil) was analyzed. The distance between the loop and coil was adjusted to improve transmission efficiency when the distance between the Tx and Rx coils was varied. In [17], the equivalent circuit model of wireless power transfer and mutual inductance theory were presented, but no detailed reason for its power and efficiency vary with the impacts of the distance, orientation, and center deviation on transmission.

In this paper, the resonant network, and the influence of coupling coefficient and the quality factor to voltage gain, current gain, and the efficiency of transfer for the bilateral compensation in wireless power transfer system are studied in detail. The parameters of the inductance coil and its compensation capacitor are designed. The formulas for the frequency bifurcation phenomenon and the mathematical modeling are given. The conditions for the occurrence of bifurcation phenomena are obtained, and the relationship between primary impedance angle and efficiency of the compensation structure is analyzed and studied. The results of Matlab simulation demonstrate the validity of the theory.

Near-field loosely coupled transformer model

Near-field wireless power transfer systems deliver power from one or more transmitting antennas to one or more receiving antennas by magnetic or electric coupling of the antennas. Receiving antennas are located in the near-field region of transmitting antennas. Operating frequencies of near-field transfer systems are in the range of 10 kHz to 100 MHz and wavelengths of such systems are from 3m to 30km. The near-field region varies from 50cm to 5km depending on the operating frequency. In case of 10 MHz operating frequency, near-field region extends to the distance of 4.8m. So if the operating frequency of a system is 10 MHz and the distance of transmitter and receiver is shorter than 4.8m, it is considered a near-field power transfer. The boundary of this region is $0.62\sqrt{D^3/\lambda}$, where D is the maximum dimension

of the antenna, and λ is the wavelength of the electromagnetic fields. If D << λ, near-field region boundary is approximated to $\lambda / 2\pi$.

Figure 1 shows a diagram of a resonant magnetically coupling system wherein a signal generator delivers power to load or device. Our experimental realization of the scheme consists of two self-resonant coils. One coil consists of a single turn drive loop and a multi-turn spiral coil, is coupled inductively to an oscillating circuit. When the RF amplifier powers the drive loop the resulting oscillating magnetic field excites the Tx coil which stores energy in the same manner as a discrete LC tank. The receive side functions in a similar manner, although a load replaces the power source, the Rx coil is coupled inductively to a resistive load. Self-resonant coils rely on the interplay between distributed inductance and distributed capacitance to achieve resonance.

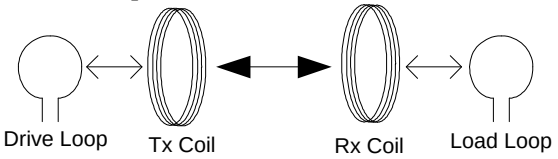

Figure 1. Magnetically coupled resonant wireless power system

A commonly-used loosely coupled transformer model, the electrical circuits of the four resonant systems are shown in Figure 2. R_1 and R_2 are equivalent series resistances of the transmitter and receiver coils. C_1 and C_2 are compensating capacitors and R_L is load resistance.

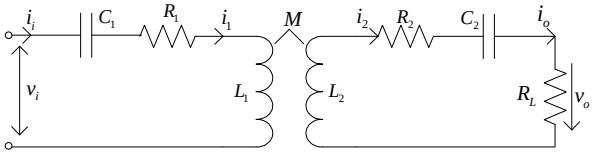

Figure 2. The electrical circuit of the four basic topologies

High reactive power at the transmitter and receiver resonant tank leads to lower power factor because of high working frequencies, so the capacitor needs to be added to compensate. The fundamental component approximation is sufficiently accurate for a high quality factor resonant circuit that works near resonance. The working frequency will deviate from the resonant frequency when the system parameters change. In order to make the imaginary part of the load impedance at the secondary resonant frequency is zero, usually use the primary capacitor to compensate the primary inductance coil and reflect reactance.

The primary loop is decoupled from the secondary loop. We have the secondary reflected impedance

$$Z_r = \frac{\omega^2 M^2}{Z_s} \tag{1}$$

Where, Z_s is the impedance of the secondary network. Ignore equivalent series resistances of the coils, in the secondary series compensate we have

$$Z_s = R_L + \mathrm{j}\omega L_2 + \frac{1}{\mathrm{j}\omega C_2} \tag{2}$$

We have got the reflected impedance of series compensation as shown

$$Z_r = \frac{\omega^4 C_2^2 M^2 R_L}{(1-\omega^2 C_2 L_2)^2 + \omega^2 C_2^2 R_L^2} + \mathrm{j}\frac{\omega^3 C_2 M^2 (1-\omega^2 C_2 L_2)}{(1-\omega^2 C_2 L_2)^2 + \omega^2 C_2^2 R_L^2} \tag{3}$$

In the primary series compensate, the input impedance looking in to the networks can be written as follows:

$$Z_{in} = \frac{1}{\mathrm{j}\omega C_1} + \mathrm{j}\omega L_1 + Z_r \tag{4}$$

$$Z_{in} = \mathrm{j}\omega L_1 + \frac{1}{\mathrm{j}\omega C_1} + \frac{\omega^4 C_2^2 M^2 R_L}{(1-\omega^2 C_2 L_2)^2 + \omega^2 C_2^2 R_L^2} + \mathrm{j}\frac{\omega^3 C_2 M^2 (1-\omega^2 C_2 L_2)}{(1-\omega^2 C_2 L_2)^2 + \omega^2 C_2^2 R_L^2} \tag{5}$$

The real part of Z_{in} is

$$\mathrm{Re}(Z_{in}) = \frac{\omega^4 C_2^2 M^2 R_L}{(1-\omega^2 C_2 L_2)^2 + \omega^2 C_2^2 R_L^2} \tag{6}$$

The imaginary part of Z_{in} is

$$\mathrm{Im}(Z_{in}) = \omega L_1 - \frac{1}{\omega C_1} + \frac{\omega^3 C_2 M^2 (1-\omega^2 C_2 L_2)}{(1-\omega^2 C_2 L_2)^2 + \omega^2 C_2^2 R_L^2} \tag{7}$$

The primary input impedance angle can be expressed as

$$\alpha = \arctan\frac{\mathrm{Im}(Z_p)}{\mathrm{Re}(Z_p)} \tag{8}$$

$$\alpha = \arctan\frac{(\omega^2 L_1 C_1 - 1)(1-\omega^2 L_2 C_2)^2 + \omega^2 C_2^2 R_L^2 (\omega^2 L_1 C_1 - 1) + \omega^4 C_2 C_1 M^2 (1-\omega^2 L_2 C_2)}{\omega^5 C_2^2 C_1 M^2 R_L} \tag{9}$$

The resonant frequency and the coupling coefficient is given by

$$\omega_0 = \frac{1}{\sqrt{L_1 C_1}} = \frac{1}{\sqrt{L_2 C_2}} \tag{10}$$

$$k = \frac{M}{\sqrt{L_1 L_2}} \tag{11}$$

The ratio of the ω and ω_0 denotes the resonant frequency of the size deviation, as shown

$$\omega_n = \frac{\omega}{\omega_0} \tag{12}$$

The secondary quality factor is

$$Q_s = \frac{\omega_0 L_2}{R_L} \tag{13}$$

Where $L_1 = L_2$。

By Kirchhoff's voltage law can determine the current equation as follows:

$$\begin{aligned} i_1(R_S + R_1 + j\omega L_1 + \frac{1}{j\omega C_1}) + j\omega i_2 M = V_i \\ i_2(R_L + R_2 + j\omega L_2 + \frac{1}{j\omega C_2}) + j\omega i_1 M = 0 \end{aligned} \tag{14}$$

Ignore the coil resistance, voltage and current gain are expressed as

$$G_v = \left|\frac{v_0}{v_i}\right| = \frac{k\omega_n^3}{\sqrt{\omega_n^2(1-\omega_n^2)^2 + (Q_S(1-\omega_n^2)^2 - k^2 Q_S \omega_n^4)^2}} \tag{15}$$

$$G_i = \left|\frac{i_0}{i_i}\right| = \frac{kQ_s\omega_n^2}{\sqrt{Q_s^2(1-\omega_n^2)^2 + \omega_n^2}} \tag{16}$$

Where, $\omega_n = \frac{\omega}{\omega_0}$ is working frequency deviates from the resonant frequency of the size.

Using formula (15) and (16), we have transmission efficiency is

$$\eta = \left|\frac{v_o i_o}{v_i i_i}\right| = G_v G_i \tag{17}$$

Taken the ω_n, k and Q_s into formula (9), we can get

$$\alpha = \arctan\frac{(\omega_n^2-1)^3 Q_s^2 + (\omega_n^2-1)\omega_n^2 + k^2 Q_s^2 \omega_n^4 (1-\omega_n^2)}{\omega_n^5 Q_s k^2} \tag{18}$$

From (18), the primary impedance angle is related to the operating frequency, the secondary factor and the coupling coefficient.。

When the $Q_s = 1,5,10,50$, the relation between angle of impedance and coupling coefficient as shown in Figure 3.

From figure 3, when the Q_s is constant, the frequency of the primary impedance angle for zero from one to three and the maximum value of primary impedance angle decreases with k increasing, that means the circuit has a frequency bifurcation phenomenon. From figure 3, we also can get that the more prone frequency bifurcation with the Q_s increasing. When K is the same, the primary impedance angle for zero from one to three with Q_s increasing, and the value of the coupling coefficient of the frequency bifurcation phenomenon becomes small.

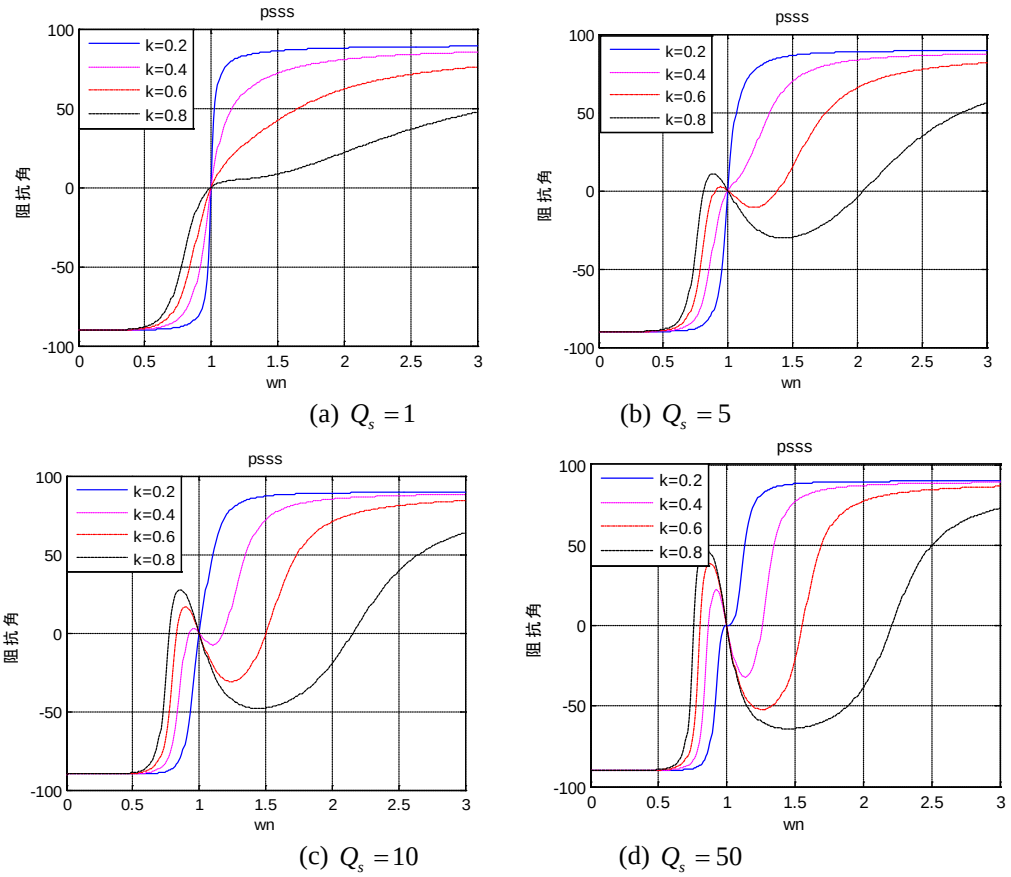

(a) $Q_s = 1$ (b) $Q_s = 5$

(c) $Q_s = 10$ (d) $Q_s = 50$

Figure 3. The relation between angle of impedance and coupling coefficient

Parameters of resonant system

The magnetic field and quality factor of Coil determines the distance and efficiency of energy transmission in the Resonant system. Transmitting coil in the form of a hollow cylindrical coil inductance made up of copper wire wound because the magnetic field of the hollow cylindrical coil winding produced per unit volume maximum. At high frequencies, the equivalent circuit model of the hollow cylindrical inductive coil shown in Figure 4.

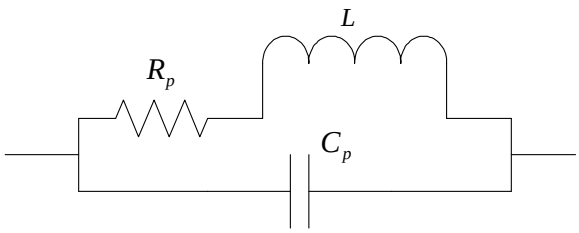

Figure 4. The equivalent model of high-frequency inductor coils

Where R_p is AC equivalent series resistance of the coil, including heat resistance R_{ohm} and radiation resistance R_{rad}, C_p is distributed capacitance. The parameters are calculated by

$$L = \mu_0 a N^2 (\ln\frac{8a}{b} - 2) \quad (19)$$

$$R_{rad} = 31171 N^2 (\frac{S^2}{\lambda^4}) \quad (20)$$

$$R_{ohm} = \sqrt{\frac{\omega\mu_0}{2\sigma}}\frac{Na}{b} \quad (21)$$

$$R_p = R_{ohm} + R_{rad} \quad (22)$$

$$C_p = \frac{2\pi^2 a\varepsilon_0}{(N-1)\ln(p/2b + \sqrt{(p/2b)^2 - 1})} \quad (23)$$

Where $\sigma = 5.8\times10^7 \,\mathrm{S/m}$, $\mu_0 = 4\pi\times10^{-7}$, $\varepsilon_0 = 8.85\times10^{-12}\,\mathrm{F/m}$, $p = 2b$, N is coil turns, a is coil radius, b is wire radius, S is coil section area, λ is wavelength.

Ignore C_p, unloaded quality factor of the coil is given by

$$Q = \frac{\omega L}{R_p} \quad (24)$$

At the resonant frequency, Take (19)-(23) in to (24), we have

$$Q(f_0, a, b, N) = \frac{2\pi f_0 \mu_0 a N^2 (\ln\frac{8a}{b} - 2)}{(\frac{\pi f_0 \mu_0 N^2 a^2}{\sigma b^2})^{1/2} + 31171 N^2 (\frac{S^2}{\lambda^4})} \quad (25)$$

From figure 5, we have the relationship of Q、radius a and turns N.

The quality factor Q increases linearly with the increase of the number of turns N and impact of the coil radius a of the quality factor Q only if N is relatively large obvious.

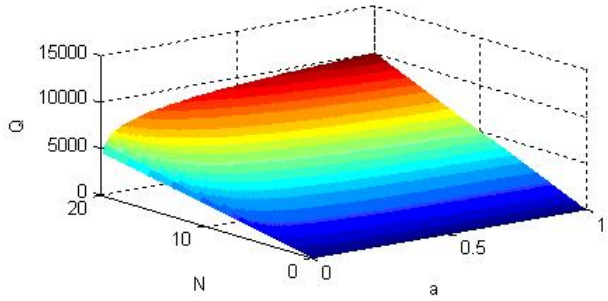

Figure 5. The relationship of Q, radius a and turns N

Coil Q value with wire radius b, frequency f trend as shown in figure 6. It is well-known that skin and proximity effects have significant impact on the current distribution and equivalent series resistance of an inductor at AC operation. The skin effect is a phenomenon in which the current density in a conductor tends to concentrate to the surface of the conductor and thus increase power loss as the operating frequency increases. Quality factor first increases with increasing frequency and wire radius, but it will drop by the impact of the skin effect when AC resistance increases faster than frequency, in this area wire radius is also bad to Q value.

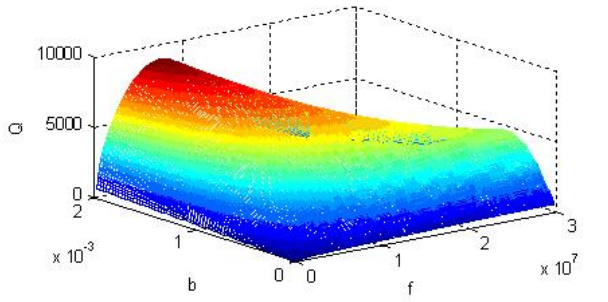

Figure 6. The relationship of Q, wire radius b and frequency f

The magnetic field strength of the coil axis to the center distance of X is calculated by equation (19), where Radius of single turn coil is a, I is Constants.

$$H(x,a) = \frac{I\cdot a^2}{2\sqrt{(a^2+x^2)^3}} \quad (26)$$

The curve between the coil radius and the magnetic field strength when the transmission distance is 10cm, 20cm, 30cm and 40cm as shown in figure 6. From figure 7 we can see that the optimal coil radius values were 15cm, 30cm, 45cm and 60cm.

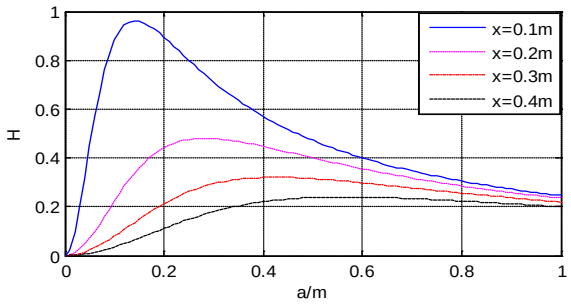

Figure 7. The curve of the radius of coils and the magnetic field intensity

$$f = \frac{1}{2\pi\sqrt{LC}} \qquad (27)$$

Combined with the actual situation to determine the parameters of the transmitting coil is , $N = 6, b = 1\text{mm}$. By formula (19) can be obtained $L \approx 14.9\mu\text{H}$. When the frequency of the high frequency inverter is 4.2MHz, according to formula (27) we can be obtained for the resonant capacitor $C = 96.5\text{pF}$.

Simulation Results and Analysis

From the above analysis, calculation and simulation results of influence of coupling coefficient and the quality factor to voltage gain, current gain, and the efficiency of transfer are given in this section. The equivalent circuit of four kinds of topology and mathematical model is simulated using Matlab.

A. *Effects of coupling coefficient and quality factor for voltage gain*

When Q_s is 5, the coupling coefficient and the voltage gain curve as shown in Figure 8.

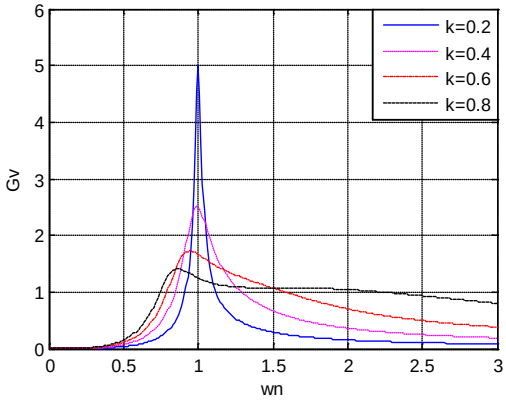

Figure 8. Curves of ω_n and voltage gain at different k

From figure 8, the coupling coefficient will affect the voltage gain and resonant frequency. We can get that voltage gain value will decrease with increasing coupling coefficient. The frequency of the voltage gain maximum points farther away from the resonant frequency with the coupling coefficient increases, and voltage gain value becomes larger but curve becomes steeper in the vicinity of the resonant frequency.

When the coupling coefficient k is 0.4, the quality factor Q_s and the voltage gain curve as shown in Figure 9.

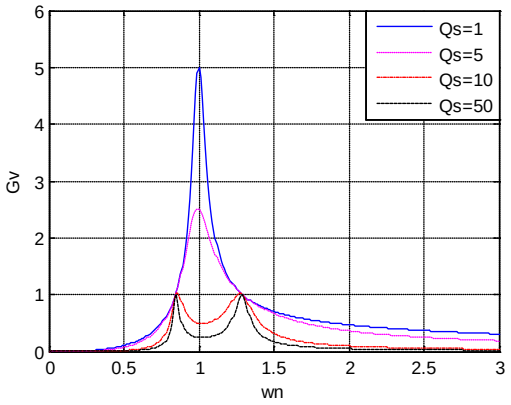

Figure 9. Curves of ω_n and voltage gain at different Q_s

From figure 9, voltage gain has two peak points with the increase of Q_s. The voltage gain decreases with the increase of Q_s , and there are two common points of the voltage gain, then independent of the voltage gain and the quality factor. Specifically, a greater impact on the voltage gain by working frequency and the curve becomes steeper with Q_s increasing.

B. *Effects of coupling coefficient and quality factor for current gain*

When Q_s is 5, the coupling coefficient and the current gain curve as shown in Figure 10.

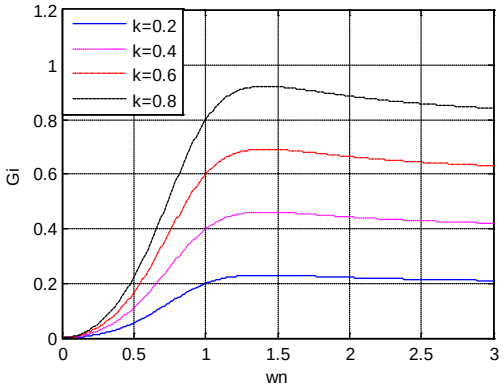

Figure 10. Curves of ω_n and current gain at different k

From figure 10, the coupling coefficient will affect the current gain and resonant frequency. We can get that current gain will decrease with decreasing coupling coefficient and the resonant frequency does not change with the variation of k. In addition, curve becomes smoother nearby the resonant frequency. This shows that the operating frequency has little effect on the current gain.

When the coupling coefficient k is 0.4, the quality factor Q_s and the current gain curve as shown in Figure 11.

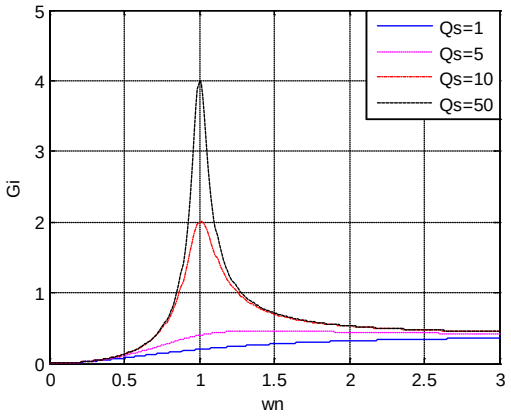

Figure 11. Curves of ω_n and current gain at different Q_s

From figure 11, current gain decreases with the increase of Q_s.

C. *Effects of coupling coefficient and quality factor for efficiency*

In the case of a constant load, when the quality factor Q_s of the secondary circuit is 5, the coupling coefficient and the transmission efficiency curve as shown in Figure 12.

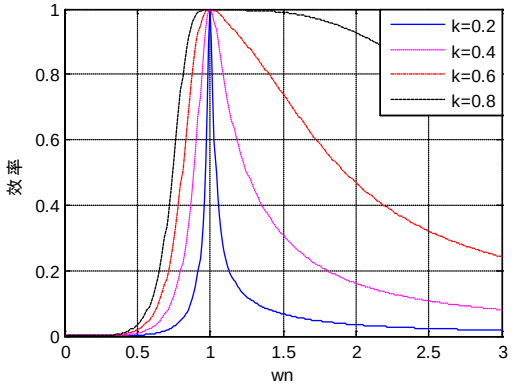

Figure 12. Curves of ω_n and efficiency at different k

From figure 12, the maximum efficiency point close to the resonance point and curves gently, the system is easy to achieve frequency tracking control. For the all compensation structure, the system transmission efficiency can reach a maximum, and the smaller the k corresponding to the curve is steep, the system operating in the frequency range of high transmission efficiency more narrow. When k is lesser, need a more accurate frequency tracking control method to ensure the system transmission efficiency is higher. In addition, when the inductance, capacitance, coupling coefficient and the input voltage is constant, with the load increases, the system will reduce the total impedance, so input and output power will increase.

When the coupling coefficient k is 0.4, the quality factor Q_s and the transmission efficiency curve as shown in Figure 13.

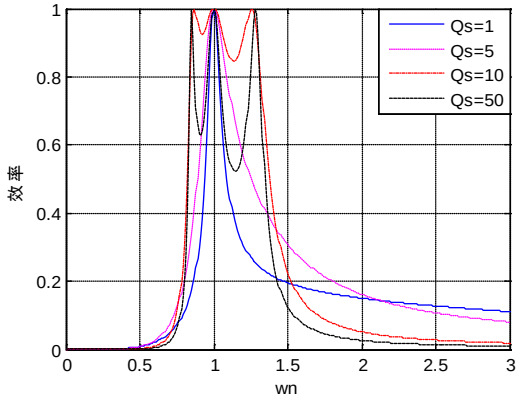

Figure 13. Curves of ω_n and efficiency at different Q_s

From Figure 13, the maximum efficiency point is from one to multiple with the increasing of the Q_s. When Q_s is too large or too small, a slight change in frequency will cause a sharp change in efficiency. Therefore, we need to appropriate Q_s value to ensure the stability of the system.

Conclusions

The topology model of resonant compensation network for wireless power transfer via magnetic coupling has been developed. The detailed mathematical derivation of the model was presented, the parameters of the inductance coil and the compensation capacitor is designed. The series-series compensation topologies are discussed in detail, analyzes the impact of the coupling coefficient and secondary quality factor for voltage gain, current gain, and the transmission efficiency, and the conditions of the frequency bifurcation phenomena caused by the load, the inductance coil, the compensation capacitor, the working frequency and the coupling coefficient are derived. The simulation results

show that the advantage of series–series compensation structure is that transmission efficiency and gain are not affected by the quality factor and the coupling coefficient, and the larger coupling coefficient and the quality factor can cause the frequency bifurcation. This paper provides the basis and reference for the following frequency tracking control.

References

1. Low, Z. N., Chinga, R. A., Tseng, R., Lin, J. (2009) Design and test of a high-power high-efficiency loosely coupled planar wireless power transfer system. *IEEE Transactions on Industry Electronics*, 56(5), p.p.1801-1812.
2. Karalis, A., Joannopoulos, J., Soljacic, M. (2008) Efficient wireless non-radiative mid-range energy transfer. *Annals of Physics*, 323(1), p.p.34-48.
3. Sallan, J., Villa, J. L., Llombart, A., Sanz, J. F. (2009) Optimal design of ICPT systems applied to electric vehicle battery charge. *IEEE Transactions on Industry Electronics*. 56(6), p.p.2140-2149.
4. Lee, S. H., Lorenz, R. D. (2011) Development and validation of model for 95%-efficiency 220-W wireless power transfer over a 30-cm air gap. *IEEE Transactions on Industry Applications*. 47(6), p.p.2495-2504.
5. Arai, S., Miura, H., Sato, F., Matsuki, H., Sato, T. (2005) Examination of circuit parameters for stable high efficiency TETS for artificial hearts. *IEEE Transactions on Power Magazine*. 41(10), p.p.4170-4172.
6. Ahn, D., Hong, S. (2013) Effect of coupling between multiple transmitters or multiple receivers on wireless power transfer. *IEEE Transactions on Industry Electronics*. 60(7), p.p.2602-2613.
7. Lee, C. K., Zhong, W.X., Hui, S.Y.R. (2012) Effects of Magnetic Coupling of Non-adjacent Resonators on Wireless Power Domino-Resonator Systems. *IEEE Transactions Power Electronics*. 27(4), p.p.1905-1916.
8. Kim, J., Son, H. C., Kim, K. H., Park, Y. J. (2011) Efficiency analysis of magnetic resonance wireless power transfer with intermediate resonant coil. *IEEE Antennas and Wireless Propagation Letters*. 45(10), p.p.389-392.
9. Luo, J., Liu, X. (2015) An approximate response of the large system with local cubic nonlinearities subjected to harmonic excitation. *Engineering Review*. 35(1), p.p.49-59.
10. Koh, K.E., Beh, T.C., Imura, T., Hori, Y. (2014) Impedance Matching and Power Division using Impedance Inverter for Wireless Power Transfer via Magnetic Resonant Coupling. *IEEE Transactions on Industry Applications*. 50(3), p.p.2061-2070.
11. Balanis, C. A. (1989) *Advanced Engineering Electromagnetics*. John Wiley & Sons: New York.
12. Kurs, A., Karalis, A., Moffatt, R. (2007) Wireless Power Transfer via Strongly Coupled Magnetic Resonances. *Science*, 317(5834), p.p.83-86.
13. Chen, L. H., Liu, S., Zhou, Y.C., Cui, T.J. (2013) An Optimizable Circuit Structure for High-Efficiency Wireless Power Transfer. *IEEE Transactions on Industry Electronics*. 60(1), p.p.339-349.
14. Sample, A. P., Meyer, D. A., Smith, J.R. (2011) Analysis, Experimental Results, and Range Adaptation of Magnetically Coupled Resonators for Wireless Power Transfer. *IEEE Transactions on Industrial Electronics*. 58(2), p.p.544-554.
15. Sasaki, K., Sugiura, S., Iizuka, H. (2014) Distance Adaptation Method for Magnetic Resonance Coupling Between Variable Capacitor-Loaded Parallel-Wire Coils. *IEEE Transactions on Microwave Theory and Techniques*. 62(4), p.p.892-900.
16. Wang, Z. H., Li, Y.P., Sun, Y. (2013) Load Detection Model of Voltage-Fed Inductive Power Transfer System. *IEEE Transactions on Power Electronics*. 11(28), p.p.5233-5243.
17. Sanghoon, C., Yong-Hae, K., Kang, S. (2011) Circuit-Model-Based Analysis of a Wireless Energy-Transfer System via Coupled Magnetic Resonances. *IEEE Transactions on Industrial Electronics*. 58(7), p.p.2906-2914.